Impact of 3D edge magnetic field configuration on divertor/SOL transport and optimization possibilities for future reactors

M. Kobayashi, K. Ida, Y. Feng[a], O. Schmitz[b,c], T.E. Evans[d], H. Frerichs[b,c], Y. Liang[c], Z.Y. Cui[e], Y. Xu[e], H.Y. Guo[f,g], D. Reiter[c], F.L. Tabares[h], D. Tafalla[h], S. Morita, N. Asakura[i], N. Ohno[j], S. Masuzaki, B.J. Peterson, K. Itoh, H. Yamada

National Institute for Fusion Science, Oroshi-cho, Toki-city, Japan
[a] Max-Planck-Institute fuer Plasmaphysik, Greifswald, Germany
[b] University of Wisconsin – Madison, Department for Engineering Physics, WI, USA
[c] Forschungszentrum Jülich GmbH, Jülich, Germany
[d] General Atomics, San Diego, California, USA
[e] Southwestern Institute of Physics, Chengdu, China
[f] Institute of Plasma Physics, Chinese Academy of Sciences, Hefei, China
[g] Tri Alpha Energy, Inc., Rancho Santa Margarita, California, USA
[h] Laboratorio Nacional de Fusion. Asociacion Euratom/Ciemat, Madrid, Spain
[i] Japan Atomic Energy Agency, Rokkasho, Aomori 039-3212 Japan
[j] Nagoya University, Nagoya, Japan

Background, motivation and final goal

➢**Helical devices:** Divertor optimization in 3D magnetic configuration is inevitable [1,2]

➢**Tokamak devices:** 2D axi-symmetric configuration + symmetry braking perturbation
→ 3D configuration
For edge transport control (Tore Supra [3], TEXTOR-DED [4]), ELM mitigation/suppression (DIII-D [5], ITER [6])

➢Recent progress of 3D numerical transport codes [7,8,9] , systematic experiments, accumulation of experimental data

➢**Identification of 3D effects** on SOL/divertor transport, **physical interpretation** & **key parameters** that control the effects, will be useful for divertor optimization in future reactors, taking full advantage of 3D configurations.

Multi-machine comparison with helical and tokamak devices.

3D effects:

Effects caused by **competition between parallel and perpendicular transport**, which originates from structural/topological change of magnetic field lines, such as **openness of stochastic field lines** due to intersection with divertor plates or formation of **magnetic island**.

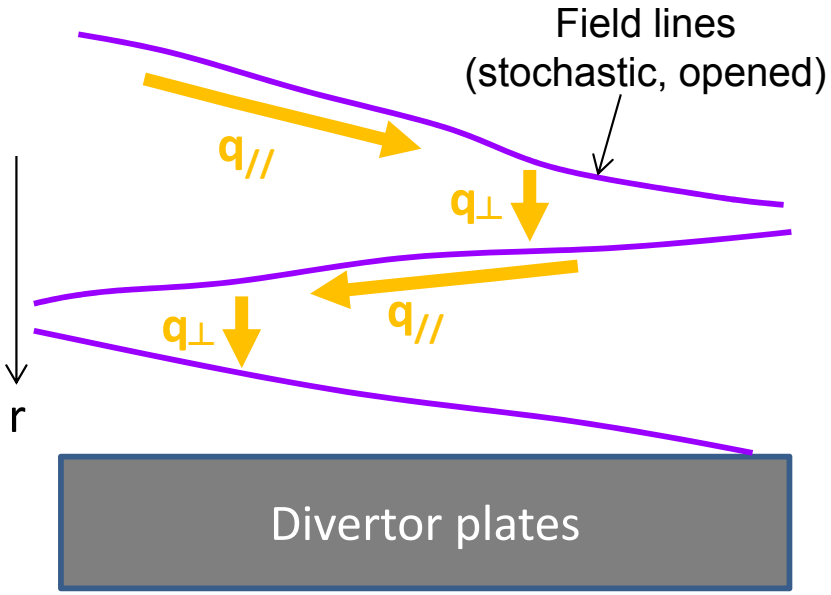

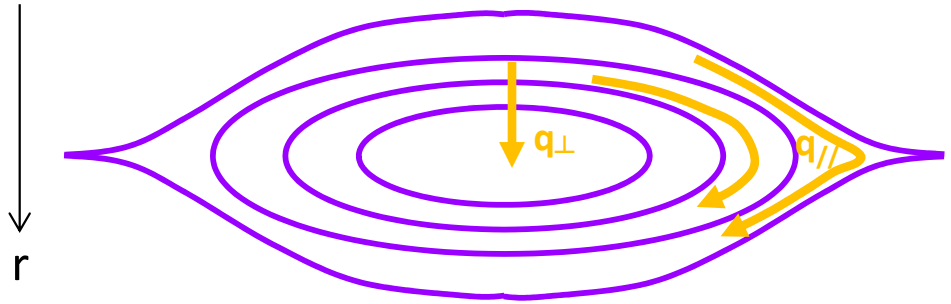

3D effect becomes significant when $q_{//}\frac{B_r}{B_t} > q_{\perp}$ **, where $q_{//}$ contributing *net* radial transport.**

Note:

$q_{//}$ in non-axisymmetric (3D) deformation of closed flux surface *does not* contribute to *net* radial transport.

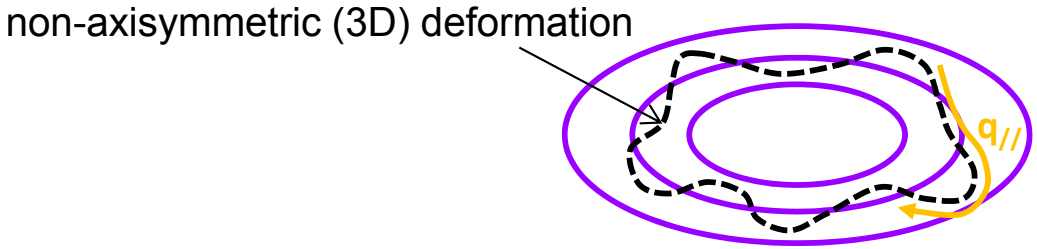

	LHD	W7-AS	W7-X	TEXTOR-DED	DIII-D	Tore Supra	ITER	HL-2A	TJ-II	EAST
R (m)	3.9	2	5.5	1.75	1.67	~2.38	6.2	1.65	1.5	1.85
a (m)	~ 0.7	~0.16	0.55	~0.46	0.60 ~ 0.67	~0.8	~2.0	0.4	~0.17	0.45
λ_{st} (width of stochastic layer) (m)	~ 0.1	~0.04 (island radial width)	~0.1 (island radial width)	~0.05 (m/n=12/4), ~0.10 (6/2), ~0.20 (3/1)	0.05 ~ 0.10 (outboard midplane)	~0.16 (20% of a)	~0.7 (90kAt, n=3), ~0.30 (45kAt, n=3), ~0.10 (strong screening), ~0.08-0.3 (M3D-C1 non-linear plasma response), 0.2 is used	0.02-0.03	~ 0.01	~ 0.02 (?)
Collisionality (SOL)	electron: 3-45 ion: 1-41			>10.0	>3		<0.05		ν_{e-} =10^5 s^{-1} ν_{i+i} =6.10^3 s^{-1}	
Collisionality				4.2 (@ r/a=0.9)	0.04 ~ 3.0 (electron pedestal)		<0.2		e-, 2.2. 10^4 s^{-1} i+i, 10^3 s^{-1}	
Mode number (RMP)	m/n=1/1			m/n=12/4, 6/2, 3/1	m/n=10/3, (m=3~15, n=1~3)	m=18+/-3, n=6	n=3, 4, m=6-14, 10/3 is used			n=1, m~4
Mode number (main structure)	m/n=2/10	m/n=9/5	m/n= (6/5), 5/5, (4/5)	axisymmetric	axisymmetric	axisymmetric	axisymmetric	axisymmetric	n/m=4/2	axisymmetric
q_{edge} @LCFS or q_{95}	1	9/5=1.8	(0.8), 1.0, (1.2)	3.6	~3.5 (3.0~4.2)	~3	3.2, 4.3, 3.2 is used	~4	0.5	3.8 ~ 4.7
L_K (m) (or $L_{//}=\pi Rq$)	10-100 (R_{ax}=3.60, 3.75, 3.90m)		37-57	~70 (m/n=12/4, I_{DED}=7kA), ~50 (12/4, 15kA), 20-35 (6/2, 7.5kA)	125 ~ 220	~10			$L_{//}=\pi Rq$=2.36m	$L_{//}=\pi Rq$=23.2m
λ_m (perpendicular characteristic scale of field line structure) (m) (or $2\pi a/m$)	~0.01				0.019 ~ 0.024, (if $2\pi a/m$ is used, 0.38 ~ 0.42)				$2\pi a/m$=0.53 (m=2)	$2\pi a/m$=0.71 (m=4)
L_C (m)		~100	~45-200	3-12 m (open field line layer)	80 ~ 200		300-1000 (open field line layer)	~20 (πqR, two limiters in HL-2A)	<L>~30m Edge, 5m SOL	
B_r (T)	2.64x(10^{-4}-10^{-3})	2.5x10^{-3}	3x10^{-3}	~10^{-3}	2.94~8.19x10^{-4} (m/n=11/3)	4.65x10^{-3}, ~3x10^{-3}	~10 x 10^-3			~ 5x10^{-4}
B_t (T)	2.64	2.5	3	1.9-2.1, 3	1.65~2.1	~3 (<4.5)	5.3	1.3-1.42	0.96	3.5
B_r/B_t	10^{-4}-10^{-3}	10^-3	10^-3	~5x10^-4	5.1~8.4x10^-4 (total), 1.4~3.9x10^-4 (m/n=11/3)	1.5x10^{-3}, ~1.0x10^{-3}	~5x10^-4 (ratio is similar as for other devices)		?	~10^{-4}
T_e (eV) @LCFS	300→150	150→20 (20-150)	200→20 (<200)	~100, 100-->40 (?)	60 ~90	~100, ~100, 100~300, ~300	4.5keV (pedestal top) 200→160 is used	20-30	30~50	
n_e (10^{19} m^{-3}) @LCFS	1→6	1→6 (<6 for 2MW)	3→6 (<3 for 10 MW)	~1, 1-->5 (?)	1.0~1.5	~1, 1.2~1.3, ~1.8, ~1	8.0 (pedestal top) 3→5 is used	0.1~0.2	0.1~0.2	
Remark					Lower triangularity: 0.26~0.65	L_K~2*pi*q*R/sigma^ 4/3 (ref.18)		For ohmic disch. (Ip~160kA, 1<ne<2e19m-3)		

Table 1: Impacts of 3D edge magnetic configurations (definitions of formulae are given in text.)

Observations	Devices	Key parameters	Interpretation	Divertor functions
$n_{div} \propto n_{LCFS}^{\alpha+1}$ $T_{div} \propto n_{LCFS}^{-\alpha}$ $\alpha = 2 \rightarrow \leq 1$ (weak div-LCFS coupling)	W7-AS [10], LHD [2], TEXTOR-DED [11,12,13]	$\tau_{m//} / \tau_{m\perp} >> 1$	//-momentum loss → $p_{LCFS} > p_{div}$	Pumping efficiency ↓ Phys. Sputtering ↑ Detach. onset density ↑ (?)
		$q_{\perp e} / q_{// e} >> 1$ $q_{// conv} / q_{// cond}$ ↗	Reduction of //-energy conduction	
Core decontamination	TEXT [14], Tore Supra [15,16], W7-AS [10], W7-X [1]†, LHD [17,18], TEXTOR-DED [19,20], TJ-II [21]	$D_{st} / D_{\perp} >> 1$	Enhanced friction force	Impurity screening ↑
		$q_{\perp i} / q_{// i} >> 1$	Ion thermal force suppression	
		$\lambda_{st-SOL} / \lambda_{imp}$ ↗	Shallow penetration of neutral impurity	
Detach. stabilization	W7-AS [22,23], LHD [24]	w_{island}	Radiation modulation by islands	Heat removal ↑
		$\Delta x_{LCFS-div}$ $\Delta x_{LCFS-island}$	Core-edge decoupling → particle fueling↓, core impurity penetration↓	
Extended density limit	TEXTOR-DED [25]	f_{RMP}	Avoidance of MARFE by RMP rotation	Density limit ↑
Footprint modification	DIII-D [26]	ν, $j_{//}$, ?	Field penetration, ?	Heat removal ↑ or ↓ (?)
Self-stochastization in LHCD	EAST [27,28]	q_{95}, ?	Helical current filament driven by LHCD	Heat removal ↑
…?				

†: numerical simulations

Divertor density regime: relation between n_{LCFS} and n_{div}, Γ_{div}, T_{div}

$n_{LCFS} \propto \bar{n}$, n_{core}

Neutral pressure $\propto \Gamma_{div}$ → pumping efficiency

$P_{rad\_div} \propto n_{div}^2$ → divertor radiation

T_{div} < 10eV → upward shift of ionization front

< 5eV → momentum loss via CX with neutrals

< 1eV → volume recombination

Relation between n_{LCFS} & n_{div}, Γ_{div}, T_{div} defines divertor performance against core plasma performance.

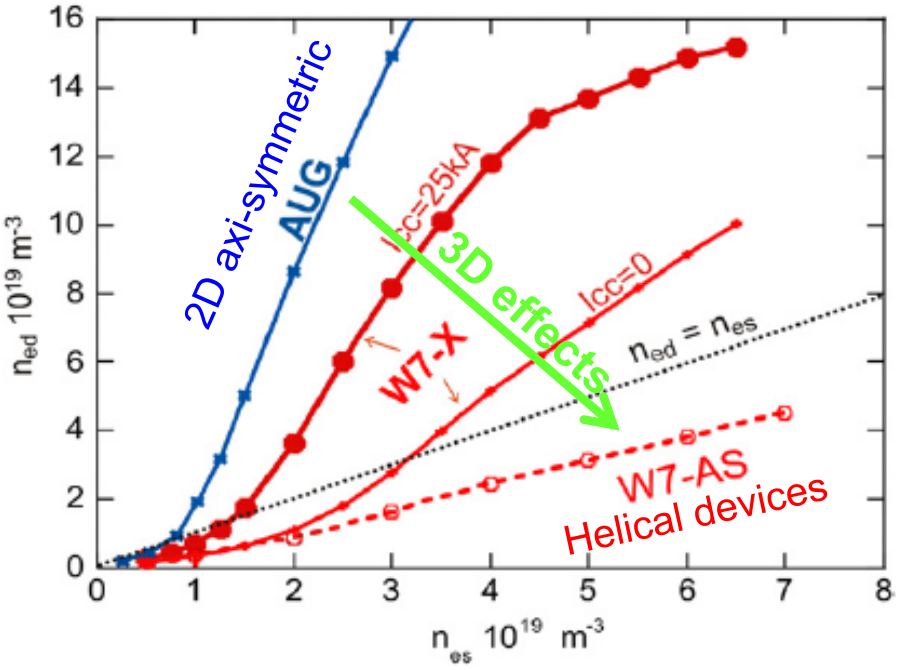

$$n_{div} \propto n_{LCFS}^{\alpha+1}$$

$$T_{div} \propto n_{LCFS}^{-\alpha}$$

$$\alpha = 2 \rightarrow \leq 1$$

3D effects → weaker coupling between LCFS & divertor

Pumping efficiency ↓
Phys. Sputtering ↑
Detach. onset density ↑ (?)

[1] Y. Feng et al., Plasma Phys. Control. Fusion **53** (2011) 024009.

Multi-machine comparison for divertor density regime

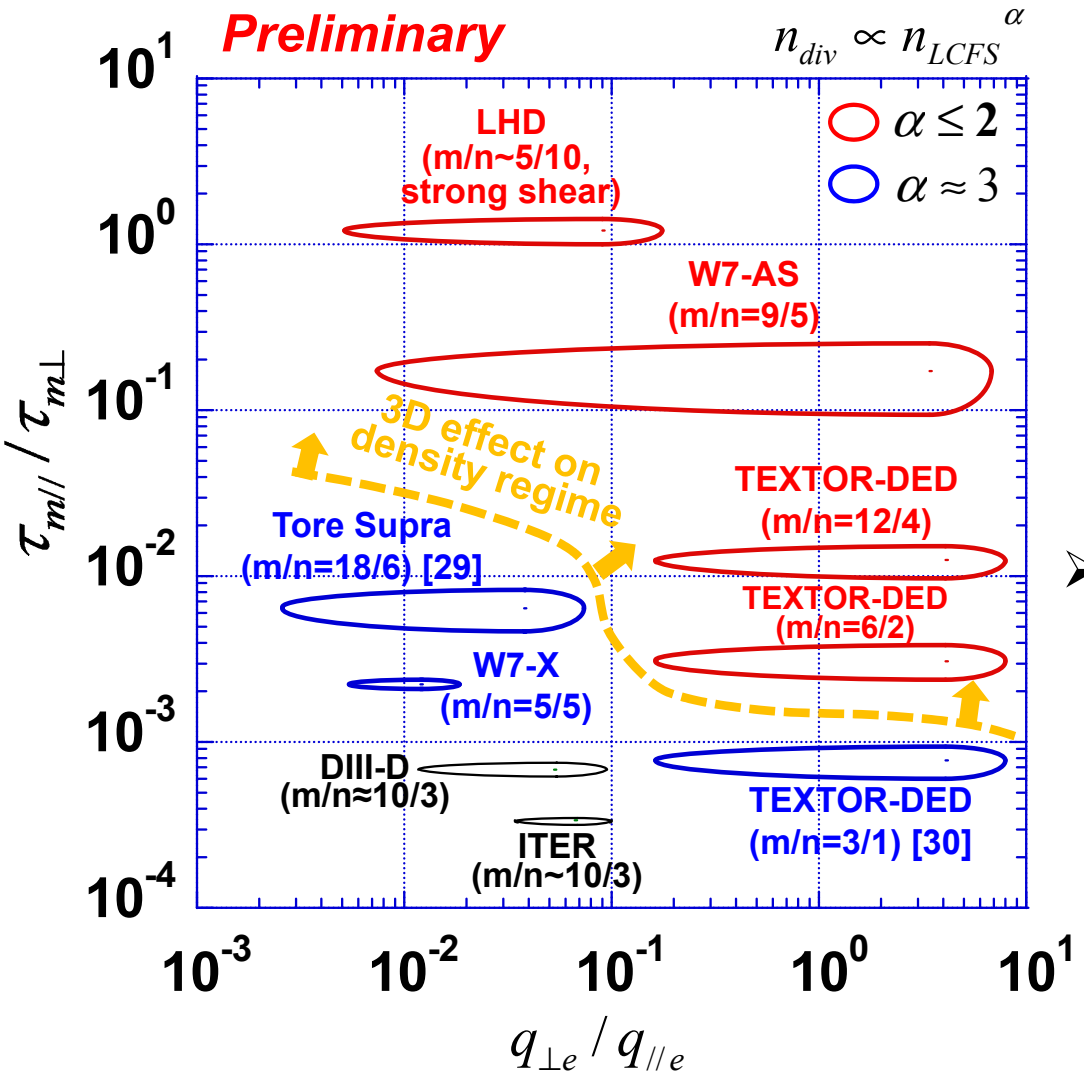

- $\perp$ loss of //-Momentum
  → //-pressure drop $p_{LCFS} > p_{div}$ [1,2]

$$\frac{\tau_{m//}}{\tau_{m\perp}} = \frac{D_{\perp} L_{//}}{V_{//} \lambda_m^{\,2}}$$

λ_m: $\perp$ characteristic scale length for momentum loss (e.g. ~2πa/m)

- Replacement of //-energy flux with $\perp$-flux (electron)
  → reduction of //-conduction energy [12]

$$\frac{q_{\perp e}}{q_{//e}} = \frac{n \chi_{\perp e}}{(B_r / B_t)^2 \kappa_{0e} T_e^{2.5}}$$

- Replacement of //-conduction energy flux with convection flux due to upstream ionization source
  → reduction of //-conduction energy [12]

$$q_{//conv} / q_{//cond}$$

[29] B. Meslin et al., J. Nucl. Mater. **266-269** (1999) 318.
[30] M. Lehnen et al., J. Nucl. Mater. **337-339** (2005) 171.

Impurity screening

Core decontamination with RMP application

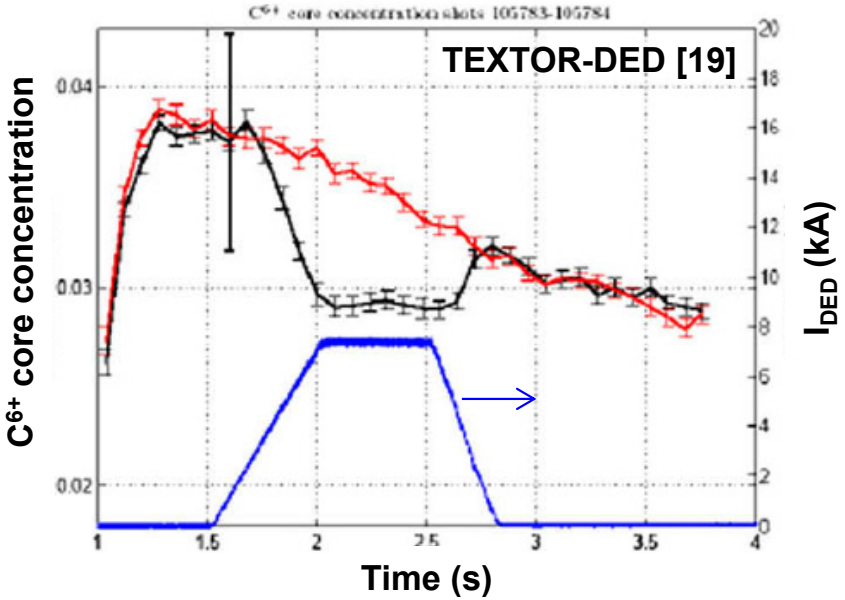

➢With B_r, outward plasma flow is enhanced
→ particle confinement time ↓
→ recycling ↑ → friction force ↑ [10, 31-35]

$$\frac{D_{st}}{D_\perp} = \frac{(B_r / B_t)^2 V_{//} L_{//}}{D_\perp}$$

➢Replacement of //-energy flux with ⊥ -flux (ion)
→ $q_{//i} = \kappa_{0i} T_i^{2.5} \nabla_{//} T_i \downarrow$ → thermal force ↓ [10]

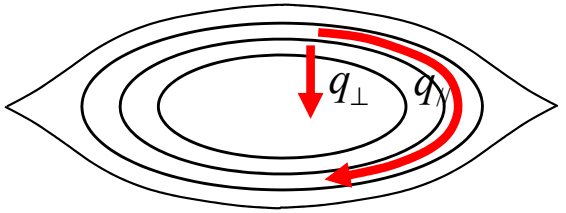

$$\frac{q_{\perp i}}{q_{//i}} = \frac{n\chi_{\perp i}}{(B_r / B_t)^2 \kappa_{0i} T_i^{2.5}}$$

//-transport model for impurity momentum

$$m_z \frac{\partial V_{z//}}{\partial t} = m_z \frac{V_{i//} - V_{z//}}{\tau_s} + 2.6 Z^2 \nabla_{//} T_i + \ldots.$$

Friction force Ion thermal force

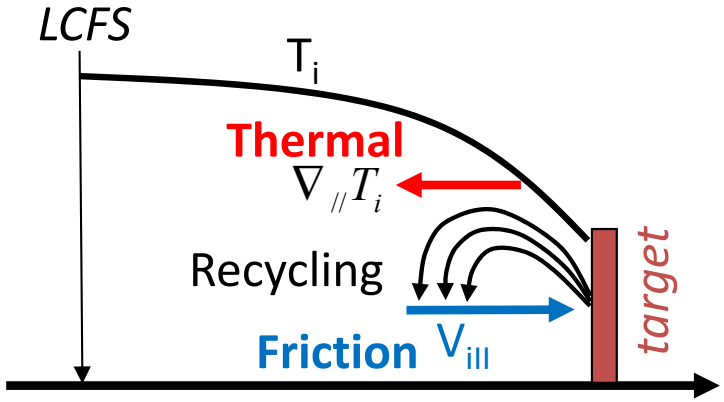

➢Thicker stochastic layer/SOL (λ_{st-SOL}) relative to neutral impurity penetration (λ_{imp})
$\lambda_{st-SOL} / \lambda_{imp}$ ↑→ better screening [36]

Multi-machine comparison for impurity screening

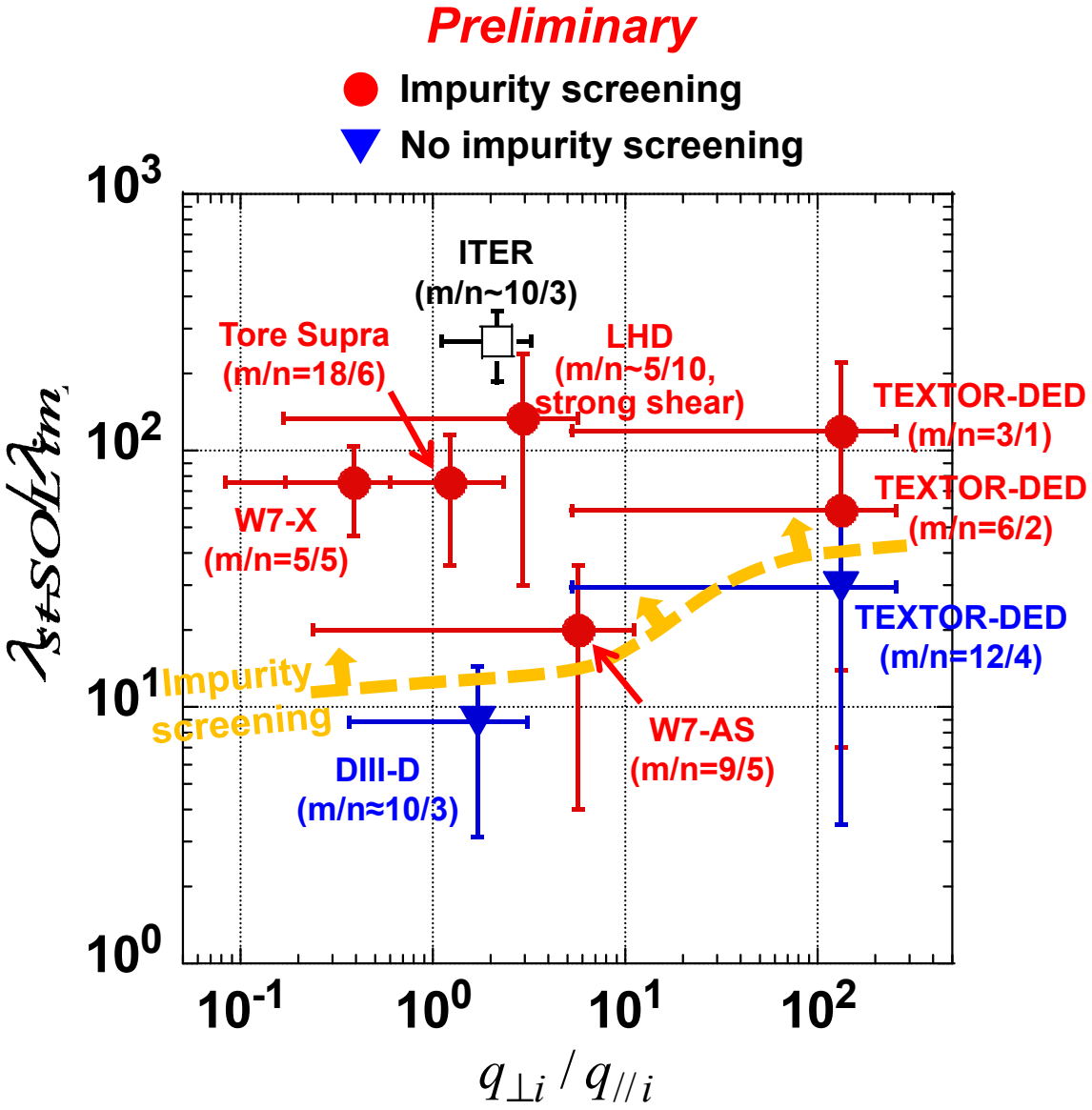

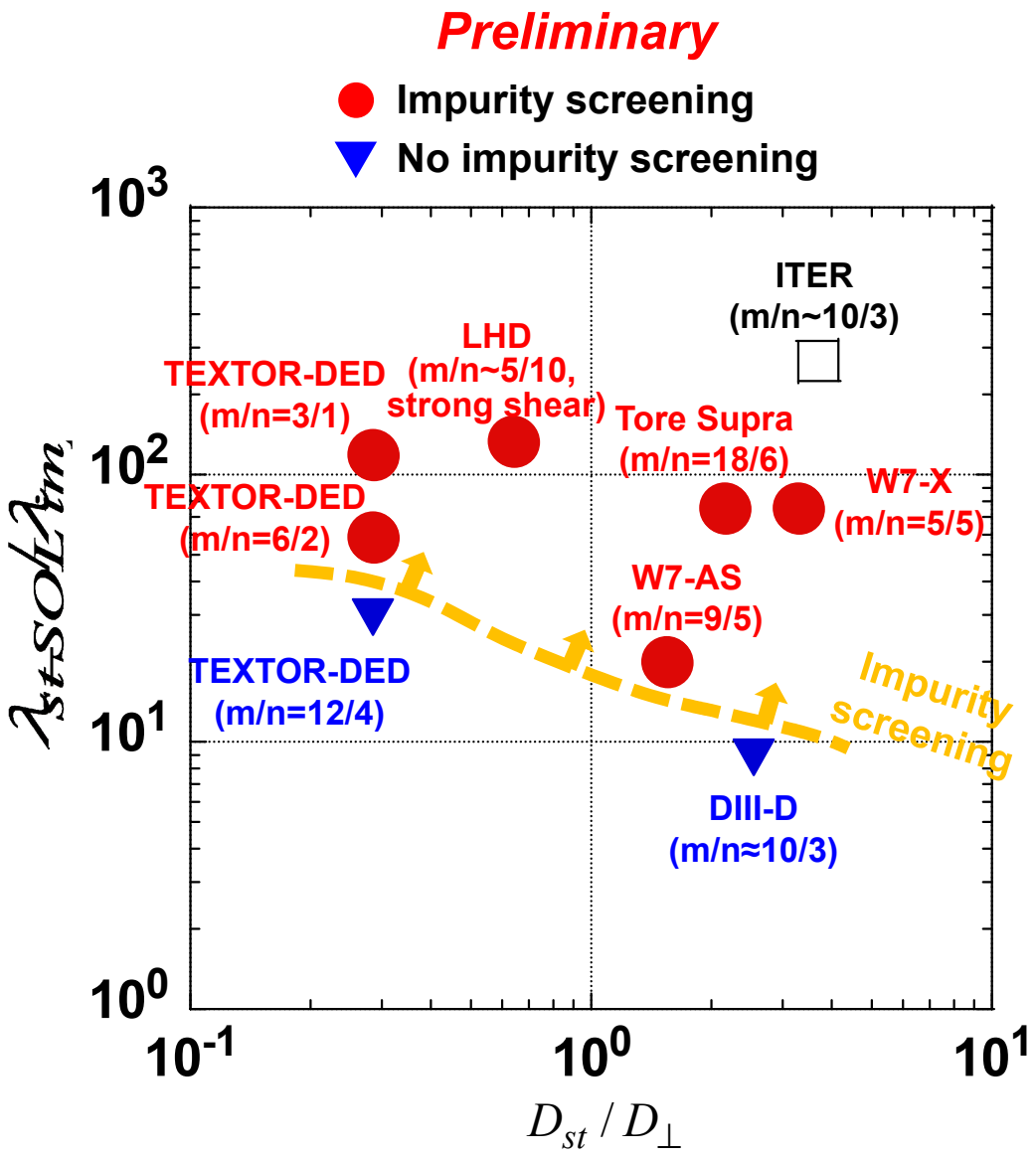

Hidden parameters characterizing impurity transport ?
Injection energy, recycle or non-recycle species [3], drift, source location [17] etc.

Detachment stabilization with RMP application (LHD)

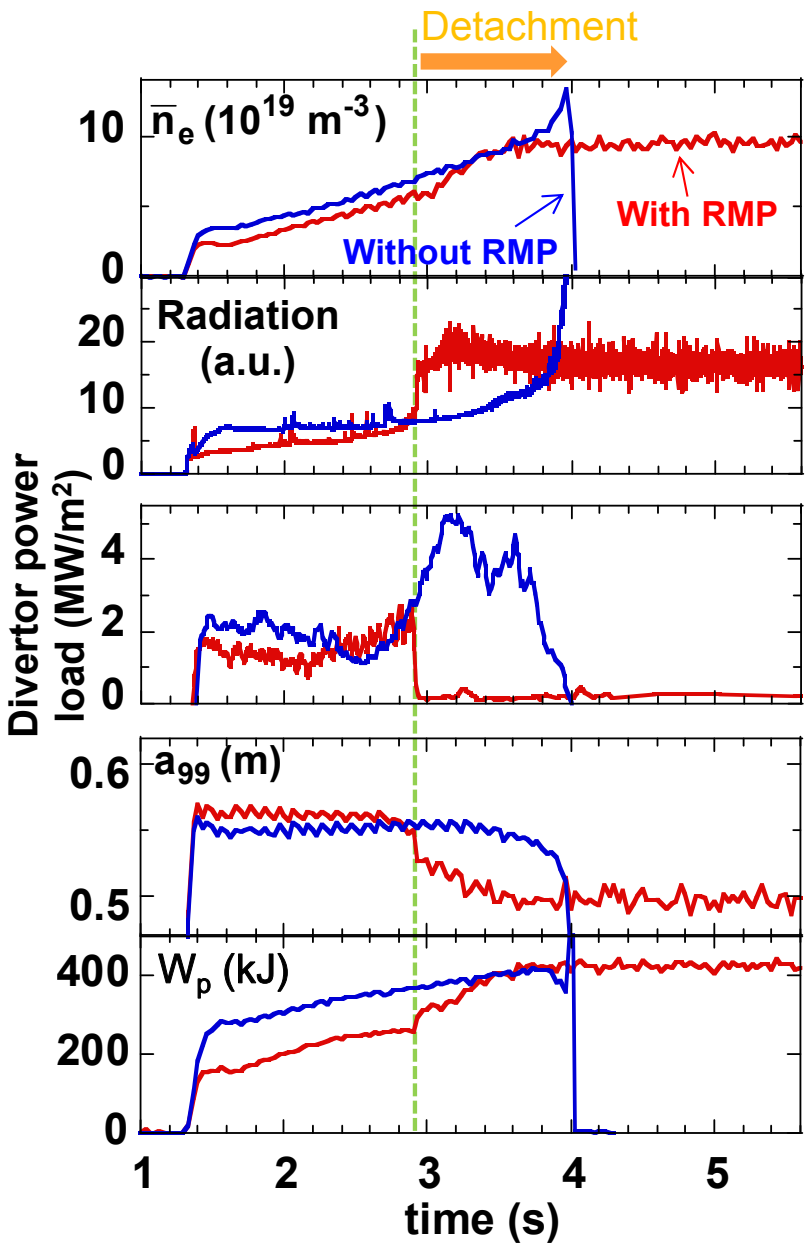

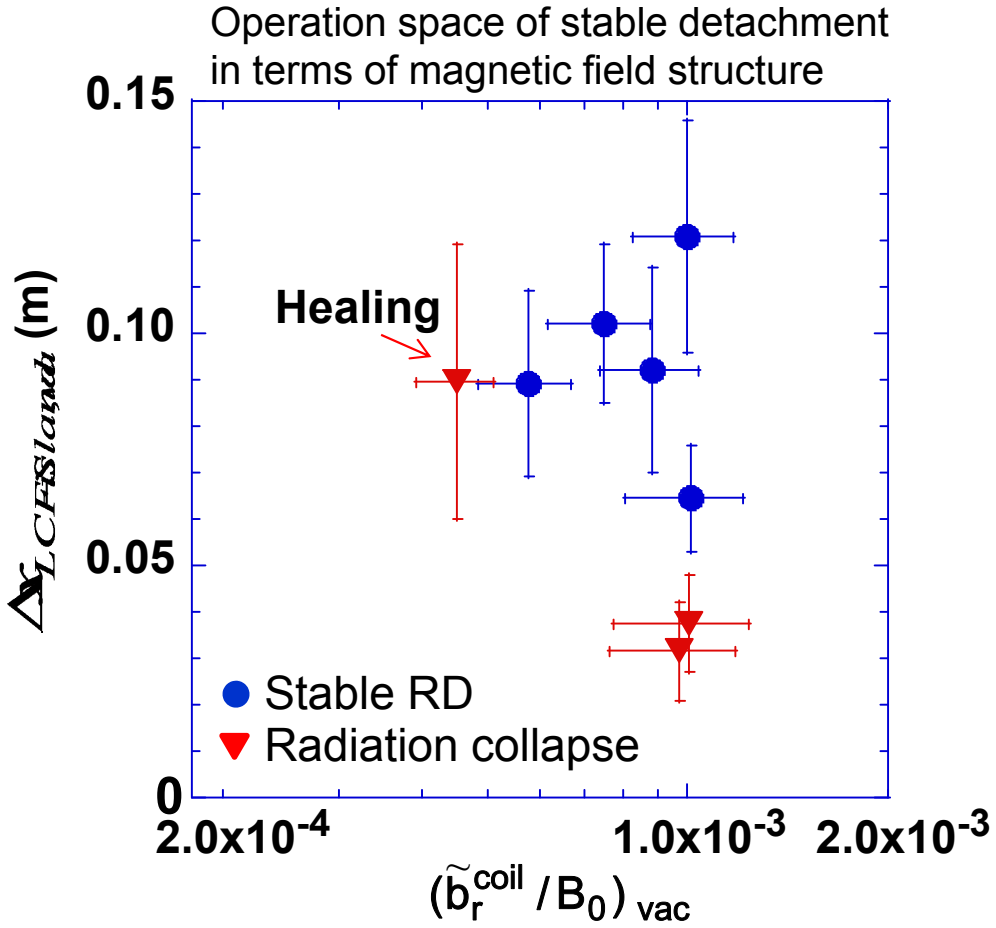

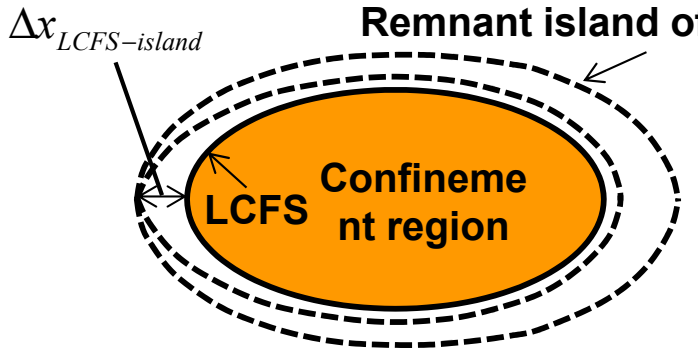

- Lower threshold of RMP strength depends also on MHD plasma response
- Separation between radiation region (island) & confinement region is important factor for stable detachment
  ←Radial extension of radiation region ~ several cm

[24] M. Kobayashi et al., Nucl. Fusion **53** (2013) 093032.

Possibility of 3D edge radiation structure control and radiation stabilization

W7-AS Δx (distance : LCFS↔divertor plate) large → stable detachment

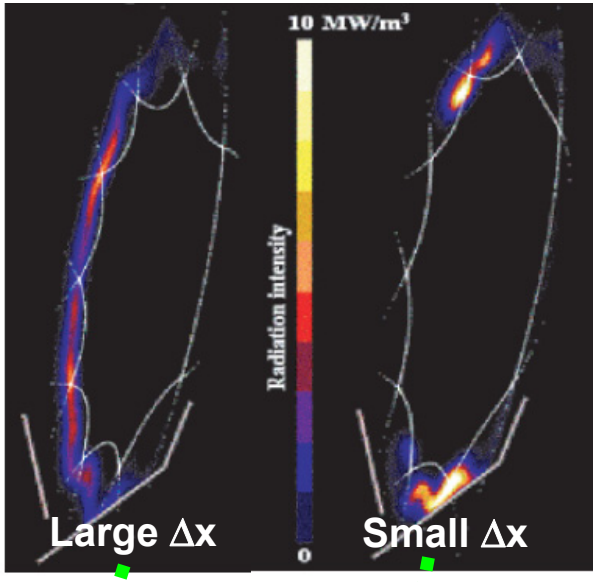

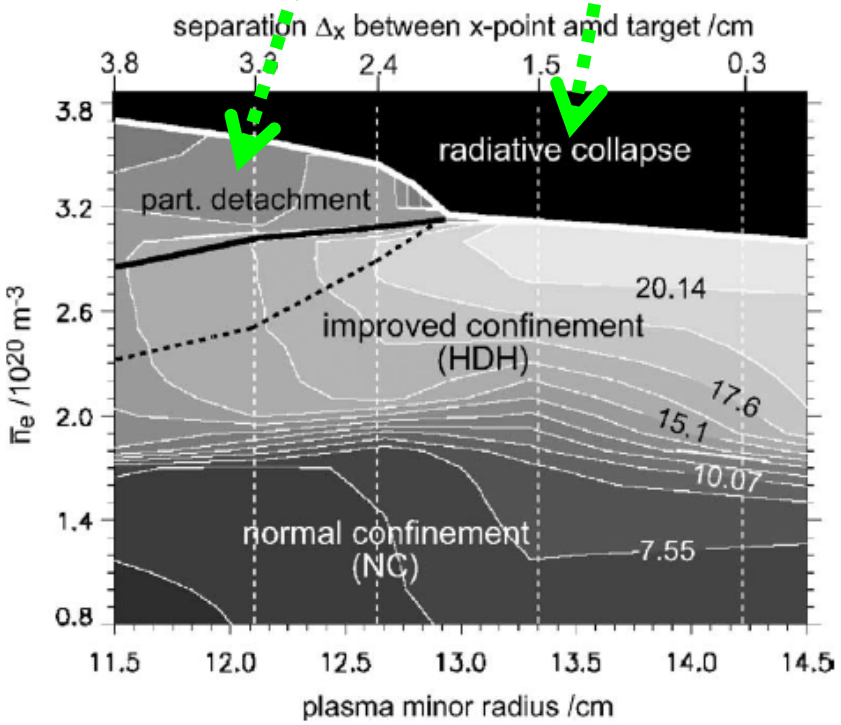

TEXTOR-DED Rotating RMP
→ density limit increased（Avoiding MARFE）

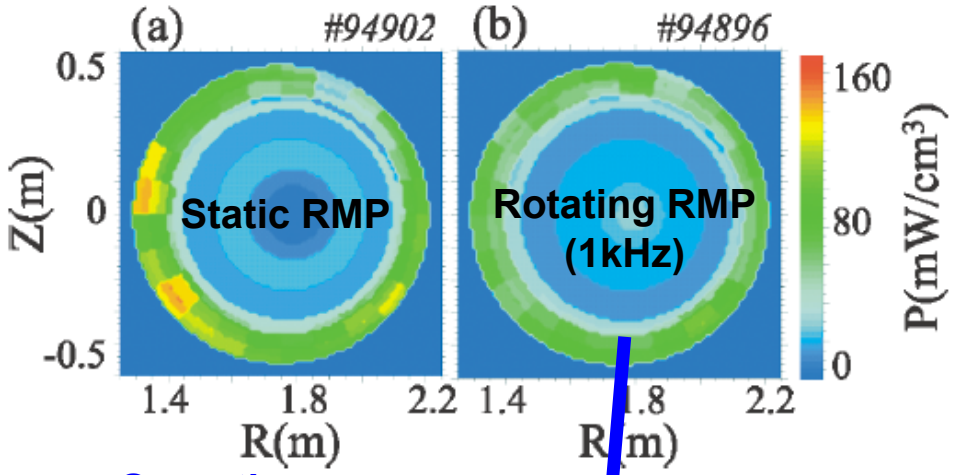

Operation space
extended up to $1.11n_e^{GW}$

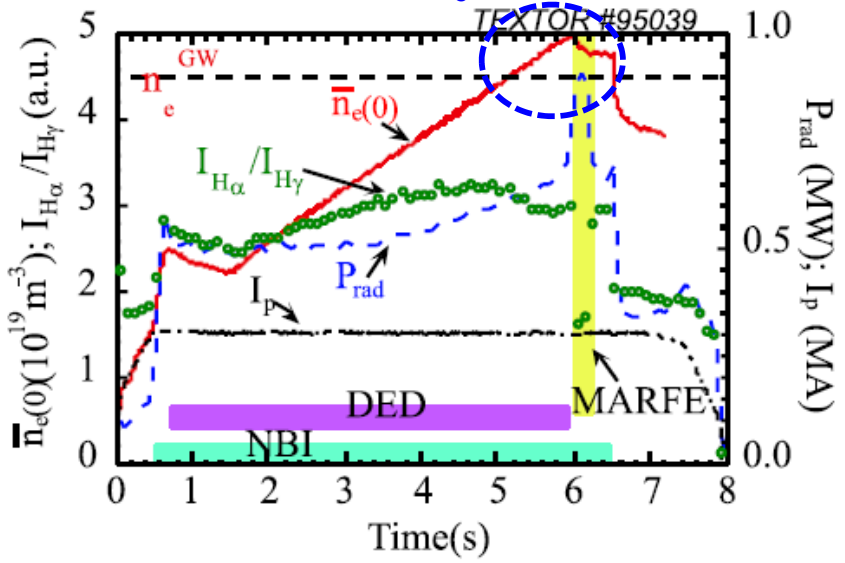

[22] P.Grigull et al. JNM **313-316** (2003) 1287. [23] Y. Feng et al., NF **45** (2005) 89.
[25] Y. Liang et al., PRL **94** (2005) 105003.

Summary

Overview of recent progress on the experimental identification and physics interpretation of 3D effects of magnetic field geometry/topology on divertor transports is undertaken.

➢**The 3D effects** : competition between transports parallel (//) and perpendicular (⊥) to magnetic field, in open field lines or magnetic islands.

➢**The competition process affects energy, particle and momentum transport in divertor/SOL region**
→ strong impacts on divertor functions: density regime, impurity screening, and detachment stability.

➢**Key parameters governing 3D transport physics** are discussed
→ still need search for missing parameters
(turbulence, electric field & current etc ?)

Systematic understandings of the impact of 3D edge magnetic field in terms of key parameters (e.g. in table 1) will open new perspective on divertor optimization for future reactors, which is not available in the 2D axi-symmetric configuration.

Further investigation with multi-machine comparison, which enables parameter scan study in substantial range, is mandatory.

“Edge Studies on HSX”, A.Bader (U.Wisconsin)

- Langmuir probe measurements of the edge and comparisons to EMC3-EIRENE.
- Strike point mapping studies. (calculations and experimental plans)
- Simulations of various edge configurations, looking at the role of islands on edge physics.

"Toroidal asymmetries in the edge of TJ-II”, F.L.Tabares (CIEMAT)

- Natural and induced asymmetries in the edge of TJ-II.
  - Localized effects of limiter insertion, edge currents
  - Analysis of edge conductivity in relation to neutral density and connection length in the SOL.
- Island divertor efficiency in TJ-II.
- Ongoing experiments.

References

[1] Y. Feng et al., Plasma Phys. Control. Fusion **53** (2011) 024009.
[2] M. Kobayashi et al., Fusion Sci. Technol. **58** (2010) 220.
[3] Ph. Ghendrih et al., Nucl. Fusion **42** (2002) 1221.
[4] O. Schmitz et al., Nucl. Fusion **48** (2008) 024009.
[5] T.E. Evans et al., Nucl. Fusion **53** (2013) 093029.
[6] O. Schmitz et al., J. Nucl. Mater. **438** (2013) S194.
[7] Y. Feng et al., PET 2013.
[8] G. Ciraolo et al., PET 2013.
[9] P. Tamain et al., J. Computational Physics **229** (2010) 361.
[10] Y. Feng et al., Nucl. Fusion **46** (2006) 807.
[11] M. Clever et al., Nucl. Fusion **52** (2012) 054005.
[12] H. Frerichs et al., Nucl. Fusion **52** (2012) 023001.
[13] M.Z. Tokar et al., Phys. Plasmas **11** (2004) 4610.
[14] S. Lippmann et al., Nucl. Fusion **31** (1991) 2131.
[15] C. Breton et al., Nucl. Fusion **31** (1991) 1774.
[16] Y. Corre et al., Nucl. Fusion **47** (2007) 119.
[17] M. Kobayashi et al., Nucl. Fusion **53** (2013) 033011.
[18] S. Morita et al., Nucl. Fusion **53** (2013) 093017.
[19] G. Telesca et al., J. Nucl. Mater. **390-391** (2009) 227.
[20] M. Lehnen et al., Plasma Phys. Control. Fusion **47** (2005) B237.
[21] I. Garcia-Cortes et al., Fusion Sci. Technol. **50** (2006) 307.
[22] P. Grigull et al. J. Nucl. Mater. **313-316** (2003) 1287.
[23] Y. Feng et al., Nucl. Fusion **45** (2005) 89.
[24] M. Kobayashi et al., Nucl. Fusion **53** (2013) 093032.
[25] Y. Liang et al., Phys. Rev. Lett. **94** (2005) 105003.
[26] T.E. Evans et al., Journal of Physics: Conference Series **7** (2005) 174–190.
[27] J. Li et al., Nature Physics **9** (2013) 817.
[28] Y. Liang et al., Phys. Rev. Lett. **110** (2013) 235002.
[29] B. Meslin et al., J. Nucl. Mater. **266-269** (1999) 318.
[30] M. Lehnen et al., J. Nucl. Mater. **337-339** (2005) 171.
[31] R. Dei-cas and A. Samain, Plasma Phys. Control. Nucl. Fusion Res. **1** (1975) 563.
[32] A.A. Shishkin , Nucl. Fusion **21** (1981) 603.
[33] A. Samain, A. Grosman and W. Feneberg, J. Nucl. Mater. **111–112** (1982) 408.
[34] A. Nicolai, F. Schoengen and D. Reiter, Plasma Phys. **27** (1985) 1479.
[35] M.Z. Tokar et al, Plasma Phys. Control. Fusion **39** (1997) 569.
[36] M.B. Chowdhuri et al., Phys. Plasmas **16** (2009) 062502.